Journal Pre-proof

Application of coumarin and coumarin-3-carboxylic acid for the determination of hydroxyl radicals during different advanced oxidation processes

Máté Náfrádi, Luca Farkas, Tünde Alapi, Klára Hernádi, Krisztina Kovács, László Wojnárovits, Erzsébet Takács

Please cite this article as: Náfrádi, Máé., Farkas, L., Alapi, Tü., Hernádi, Klá., Kovács, K., Wojnárovits, Láó., Takács, Erzsé., Application of coumarin and coumarin-3-carboxylic acid for the determination of hydroxyl radicals during different advanced oxidation processes, *Radiation Physics and Chemistry* (2019), doi: https://doi.org/10.1016/j.radphyschem.2019.108610.

This is a PDF file of an article that has undergone enhancements after acceptance, such as the addition of a cover page and metadata, and formatting for readability, but it is not yet the definitive version of record. This version will undergo additional copyediting, typesetting and review before it is published in its final form, but we are providing this version to give early visibility of the article. Please note that, during the production process, errors may be discovered which could affect the content, and all legal disclaimers that apply to the journal pertain.

Application of coumarin and coumarin-3-carboxylic acid for the determination of hydroxyl radicals during different advanced oxidation processes

Máté Náfrádi[1], Luca Farkas[1], Tünde Alapi[1], Klára Hernádi[2], Krisztina Kovács[3], László Wojnárovits[3], Erzsébet Takács[3]

[1]Department of Inorganic and Analytical Chemistry, University of Szeged, Szeged, Hungary

[2]Department of Environmental and Applied Chemistry, University of Szeged, Szeged, Hungary

[3]Institute for Energy Security and Environmental Safety, Centre for Energy Research, Budapest, Hungary
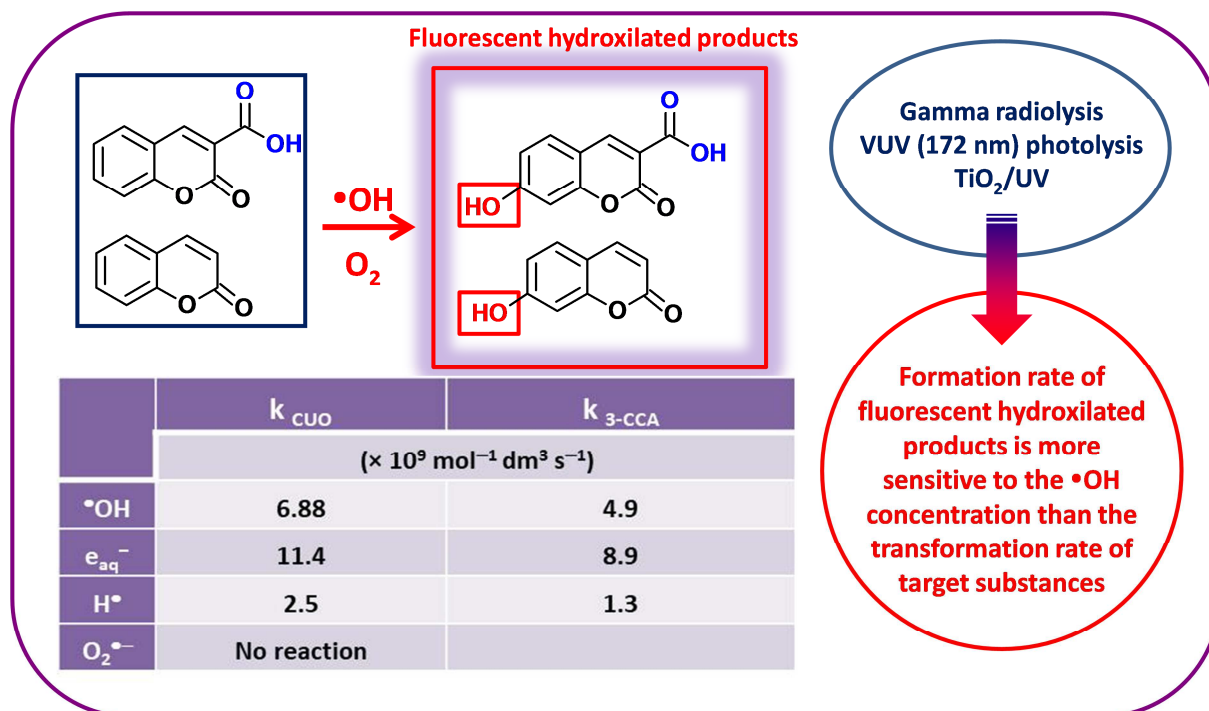
Highlights

- Rate constants of reactions with $^\bullet OH$, $H^\bullet$ and e_{aq}^- were determined

- Formation of hydroxylated fluorescent products requires $^\bullet OH$

- Reaction with $H^\bullet$ and e_{aq}^- does not results in fluorescent products

- Hydroxylated products are more sensitive to $^\bullet OH$ in bulk than coumarin

- Adsorption on TiO_2 has to be considered when evaluating $^\bullet OH$ scavenging effect

2

Graphical abstract

	k_{CUO}	$k_{3\text{-}CCA}$
	($\times 10^9$ mol^{-1} dm^3 s^{-1})	
$\bullet$OH	6.88	4.9
e_{aq}^-	11.4	8.9
H$\bullet$	2.5	1.3
$O_2^{\bullet-}$	No reaction	

Fluorescent hydroxilated products

Gamma radiolysis
VUV (172 nm) photolysis
TiO$_2$/UV

Formation rate of fluorescent hydroxilated products is more sensitive to the $\bullet$OH concentration than the transformation rate of target substances

Abstract

Transformation of coumarin (COU) and coumarin-3-carboxylic acid (3-CCA), the formation of their fluorescent hydroxylated products, (7-hydroxy-coumarin (7-HO-COU) and 7-hydroxy-3-carboxycoumarinic acid (7-HO-3-CCA)) were investigated and compared using three different advanced oxidation processes: gamma radiolysis, VUV (172 nm) photolysis and heterogeneous photocatalysis (TiO_2/UV (300-400 nm)). Beside $^\bullet OH$ (hydroxyl radical), other reactive species: $H^\bullet$ (H-atom, in VUV irradiated aqueous solution and in gamma radiolysis with low yield) and e_{aq}^- (hydrated electron, in gamma radiolysis) also contributed to the degradation.

The reaction rate constants of COU and 3-CCA with each reactive species were determined via pulse radiolysis. The values obtained were: 6.88×10^9 and 4.9×10^9 with $^\bullet OH$; 2.5×10^9 and 1.3×10^9 with $H^\bullet$; 11.4×10^9 and 14.3×10^{10} mol^{-1} dm^3 s^{-1} with e_{aq}^-, in the case of COU and 3-CCA, respectively. Based on the results of radiolysis it was suggested, that the formation of fluorescent products are initiated only by $^\bullet OH$.

The effects of dissolved O_2 and $^\bullet OH$ scavengers (MeOH and t-BuOH) were also investigated. In radiolysis dissolved O_2 increased the formation rate of fluorescent products. In VUV photolysis of COU and 3-CCA solutions the inhibition effect of alcohols was more pronounced in the presence of O_2 than in its absence. In heterogeneous photocatalysis both MeOH and t-BuOH decreased the transformation rate of COU, while they had no observable effect on that of 3-CCA, which is well adsorbed on TiO_2 surface.

4

1. Introduction

In Advanced Oxidation Processes (AOPs) generally hydroxyl radical ($^\bullet$OH) reactive intermediate plays the main role in the degradation of harmful organic pollutants. Several fluorescent probes e.g., coumarines, phenoxazine or 9-phenylxanthene (Shen et al., 1995; Villegas et al., 2005; Newton et al., 2006) have been proposed for use with scavenger methods to quantify the $^\bullet$OH yields.

Both coumarin (COU) and coumarin-3-carboxylic acid (3-CCA) (Fig. 1) have been used for the detection of $^\bullet$OH in the case of γ-radiolysis and heterogeneous photocatalysis. Reaction of COU and 3-CCA with $^\bullet$OH produces fluorescent products (7-hydroxy-coumarin (7-HO-COU) and 7-hydroxy-3-carboxycoumarinic acid (7-HO-3-CCA), respectively) (Fig. 1) with excitation bands at ~320-370 nm and ~380-400 nm, respectively, and emission maximum at ~450 nm (Manevich et al., 1997; Louit et al., 2005; Maeyama et al., 2011a, 2011b). Due to the carboxyl group in its structure 3-CCA undergoes a protonation/deprotonation equilibrium with pK_a 3.3-3.7 (Collins et al., 1994; Manevich et al., 1997).
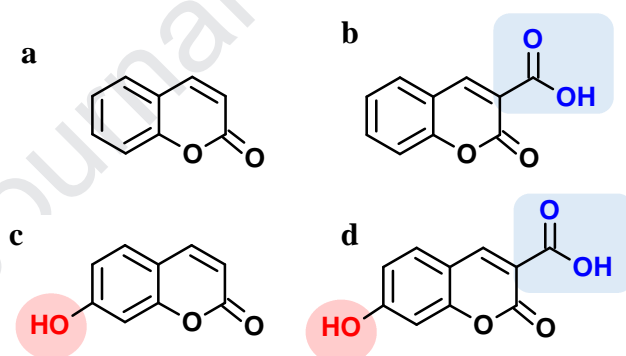
Figure 1. Structures of the investigated substances and their fluorescent hydroxylated products.

a: Coumarin (COU); b: Coumarin-3-carboxylic acid (3-CCA); c: 7-Hydroxycoumarin (7-HO-COU); d: 7-Hydroxycoumarin-3-carboxylic acid (7-HO-3-CCA)

Using radiolysis, the yield of 7-HO-COU was determined, the formation of different hydroxycoumarins and the dissolved O$_2$ dependency of 7-HO-COU formation were investigated by Louit et al., 2005. The applicability and $^\bullet$OH scavenging properties of 3-CCA during γ-radiolysis were also investigated (Manevich et al., 1997), and the reaction rate

5

constants and 7-HO-3-CCA yields were determined using competitive technics (Newton et al., 2006). The hydroxylation process and the O_2 dependency of 3-CCA was found to be similar to that of COU (Yamashita et al., 2012).

By detecting $^\bullet OH$ COU was also used to study the mechanism of photocatalysis (Czili et al., 2008; Cernigoj et al., 2009; Nosaka et al., 2014; Kakuma et al., 2015; Zhang et al., 2015; Nagarajan et al., 2017).

In the case of radiolysis, TiO_2 photocatalysis and VUV photolysis reactive intermediates other than $^\bullet OH$ also form, e.g., hydrated electron (e_{aq}^-), superoxide radical anion/perhydroxyl radical pair ($O_2^{\bullet-}/HO_2^\bullet$) or hydrogen atom ($^\bullet H$). The aim of this work was to determine their reactions with COU and 3-CCA and to check whether these intermediates also give some fluorescing product. Besides, our purpose was to compare both the reactions and the $^\bullet OH$ detection ability of 3-CCA and COU. To better understand and evaluate the results, pulse radiolysis coupled with time resolved spectroscopy was applied to determine the rate constants and mechanisms of the reactions of COU and 3-CCA with various reactive species ($^\bullet OH$, $H^\bullet$ and e_{aq}^-). Both compounds were used to evaluate the $^\bullet OH$ production during heterogeneous photocatalysis, where the different adsorption properties of COU (non-adsorbed) and 3-CCA (well adsorbed) may play important roles. COU and 3-CCA were used to investigate the $^\bullet OH$ formation rate during vacuum-ultraviolet ($VUV_{172\ nm}$) photolysis, too. Effect of dissolved O_2, MeOH and t-BuOH as $HO^\bullet$ scavengers were also investigated and compared in the case of each method, such as radiolysis, VUV photolysis and heterogeneous photocatalysis.

2. Experimental

Pulse radiolysis was conducted to observe the transient intermediates using 800 ns pulses of 4 MeV electrons, with optical detection in 1.0 cm cell, dose/pulse 20 Gy (determined using standard KSCN dosimetry) (Földiák et al., 1988).

In γ radiolysis experiments 10 mL ampoules with COU or 3-CCA solution (1.0×10^{-4} mol dm^{-3}) were placed at equal distance from the ^{60}Co γ-source of a panoramic type irradiator, to have a dose rate of 0.7 kGy h^{-1} (700 J kg^{-1} h^{-1}). The solutions were irradiated in sealed ampoules, with doses 0.05, 0.1, 0.2, 0.4, 0.6 and 1.0 kGy. The samples were saturated with O_2, N_2O or with N_2. In O_2 and N_2O containing solutions the pH was set to 7.0 with phosphate buffer. When the samples were bubbled with N_2 to eliminate dissolved O_2, pH 2.1 was set with $HClO_4$ solution and 5 v/v% t-BuOH was added as radical scavenger.

The Xe_2^* excimer lamp (Radium Xeradex^{TM}, 130 mm long, 46 mm diameter, 20 W) was centred in a high purity silica quartz envelope (53 mm diameter), which transmits the 172 nm light. The volume between the wall of the excimer lamp and the inert wall of envelope was rinsed with N_2 for cooling the lamp and avoid the decrease of VUV light intensity via absorption by O_2. The inert diameter of reactor was 68 mm, thus the thickness of irradiated water layer was 5 mm. The aqueous solution was circulated continuously (375 mL min^{-1}) between the reactor and the liquid containing reservoir. Double walled, water cooled reactor was used and the temperature was set to 25 ± 0.5 °C. Samples were taken from the reservoir. The total volume of the circulated solution was 500 mL. The photon flux emitted by the excimer lamp (20 W) at 172 ± 14 nm determined by methanol actinometry was found to be 3.0×10^{-6} mol$_{photon}$ s^{-1} (Arany et al., 2013). The solution in the reservoir was bubbled with O_2 or N_2.

In heterogeneous photocatalytic experiments the TiO_2 concentration was 1.0 g dm^{-3}. Irradiation was performed with a fluorescent UV lamp (GCL303T5/UVA, LighTech, Hungary, dimensions: 307 mm $\times$ 20.5 mm, 15 W electric input) emitting in the 300–400 nm range with $\lambda_{max} = 365$ nm. The photon flux of the light source was 7.23×10^{-6} mol$_{photon}$ s^{-1}, determined by ferrioxalate actinometry (Hatchard and Parker, 1956). The volume of the irradiated suspension was 250 mL. Since 3-CCA adsorbed well on the surface of TiO_2, before filtration 0.5 mL 0.5 mol dm^{-3} NaF solution was added to 1.0 mL suspension for desorption of both 3-CCA and 7-HO-3-CCA. By this way, both compounds were desorbed completely. To remove the photocatalyst particles, samples were centrifuged and filtered with a syringe filter (FilterBiO PVDF-L, 0.20 μm).

The transformation of COU and 3-CCA were followed using spectrophotometry (Agilent 8453). Absorbance was determined at the maximum of the spectra, 277 nm and 291 nm in the case of COU and 3-CCA, respectively. The molar absorbance of COU and 3-CCA at these wavelengths were 10300 and 12100 mol^{-1} dm^3 cm^{-1}, respectively.

Fluorescence spectroscopy (Hitachi F4500) was applied to determine the concentration of formed hydroxylated products, 7-HO-COU and 7-HO-3-CCA. Excitation wavelength for 7-HO-COU was 345 nm and pH 5.5 was set for each measurement. The determination of 7-HO-COU concentration was based on the intensity of the emitted fluorescence light at 455 nm. The 7-HO-3-CCA concentration was measured based on the intensity of the emitted fluorescence light at 447 nm. The wavelength of excitation was 387 nm. pH 9.5 was set to avoid the emission of fluorescent light from 3-CCA.
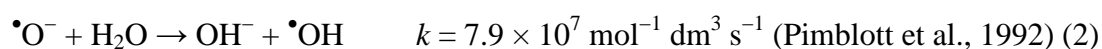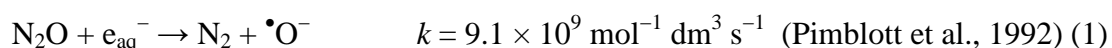
Sigma-Aldrich[®] and VWR[®] provided analytical standard for COU, 3-CCA, 7-HO-COU and 7-HO-3-CCA (> 98%). Methanol (MeOH) and *t*-buthanol (t-BuOH) were purchased from VWR[®] (HiPerSolv CHROMANORM®, super gradient grade for HPLC). NaF, HCl, NaOH, HOCl$_4$, Na$_2$HPO$_4$ and NaH$_2$PO$_4$ were obtained from Sigma-Aldrich. High purity water was prepared through Milli-Q[®] Integral Water Purification System (MerckMillipore[®]). The O$_2$ (99.5 %), N$_2$ (99.995 %) and air were provided by Messer Hungarogáz Kft. The TiO$_2$ photocatalyst (Aeroxide P25[®]) was purchased from Acros Organics.

Experiments were made in 1.0×10^{-4} mol dm^{-3} aqueous COU and 3-CCA solutions. The transformations of COU and 3-CCA were characterized by the initial rate of transformation, obtained from linear regression fits to the actual concentration versus the duration of irradiation, up to 20 % of the concentration of the transformed target compound. The formation rates of 7-HO-COU and 7-HO-3-CCA were obtained from linear regression fits to the actual concentration versus the duration of irradiation.

3. Results and Discussion

3.1. Pulse radiolysis

Using high-energy ionizing radiation (accelerated electron irradiation or γ-rays), in dilute aqueous solution the degradation of water molecules supplies the reactive intermediates that react with the solute(s) (Buxton et al., 1988; Spinks and Woods, 1990; Buxton, 2004). These intermediates and their yields are •OH 0.28 μmol J^{-1}, e$_{aq}^-$ 0.28 μmol J^{-1} and with low yield H• 0.062 μmol J^{-1}. The reactions of •OH were investigated in N$_2$O saturated solutions in order to eliminate the dissolved O$_2$ and to transform e$_{aq}^-$ to •OH in the reaction:

$$N_2O + e_{aq}^- \rightarrow N_2 + {}^{\bullet}O^- \qquad k = 9.1 \times 10^9 \text{ mol}^{-1} \text{ dm}^3 \text{ s}^{-1} \text{ (Pimblott et al., 1992) (1)}$$

$$^{\bullet}O^- + H_2O \rightarrow OH^- + {}^{\bullet}OH \qquad k = 7.9 \times 10^7 \text{ mol}^{-1} \text{ dm}^3 \text{ s}^{-1} \text{ (Pimblott et al., 1992) (2)}$$

Since both COU and 3-CCA have strong light absorption below c.a. 340 nm, the spectra were investigated above this limit. In the COU transient spectrum there are two peaks with maxima at 350 and 423 nm (pH 7.0) (Fig. 2a). The decay of the two peaks showed similarities, although, the decay of the 350 nm band looked to be somewhat faster. However, at shorter wavelengths the building-up of the final products also gave some contribution to the absorbance. Assuming that the two peaks belong to the same intermediate(s) and •OH reacts solely to give these intermediates the values of molar absorbance are estimated to be 3400 and 2000 mol^{-1} dm^3 cm^{-1}, respectively. The time dependences of the absorbance build-ups obeyed

8

the (pseudo-)first-order kinetics and pseudo-first-order rate constants linearly depended on the COU concentration. The slope yielded a second-order rate constant of 6.88×10^9 mol^{-1} dm^3 s^{-1}. Our value is in agreement with the $k_{\bullet OH}$ determined by Singh et al. (2002) also in pulse radiolysis (6.4×10^9 mol^{-1} dm^3 s^{-1}). The value of Gopakumar et al. (1977) obtained in competitive experiment is much lower (2×10^9 mol^{-1} dm^3 s^{-1}).

Table 1. Rate constants of COU and 3-CCA reactions with $^\bullet$OH, e_{aq}^-, H$^\bullet$ and $O_2^{\bullet-}$. Abbreviations: Pr. pulse radiolysis, Comp. competitive technique.

|	k^{COU} ($\times 10^9$ mol^{-1} dm^3 s^{-1})	$k^{3\text{-}CCA}$ ($\times 10^9$ mol^{-1} dm^3 s^{-1})
$^\bullet$OH	**6.88, this work, Pr.**	**4.9, this work, Pr**.
	6.4, Singh et al., 2002, Pr.	5.0±1.0, Manevich et al., 1997, Pr.
	2.0, Gopakumar et al., 1977, Comp.	5.5, Newton et al., 2006, Comp.
		6.0, Yamashita et al., 2012, Pr.
		6.8±0.2, Yamashita et al., 2012, Comp.
e_{aq}^-	**11.4, this work, Pr.**	**14.3, this work, Pr.**
	17.0, Singh et al., 2002, Pr.	20.6±0.2, Yamashita et al., 2012, Pr.
	16.0, Land and Truscott, 1979, Pr.	
H$^\bullet$	**2.5, this work, Pr.**	**1.3, this work, Pr.**
$O_2^{\bullet-}$	No reaction, Pr.	No reaction, Yamashita et al., 2012, Pr.

The transient absorption spectrum that forms in $^\bullet$OH reaction with 3-CCA (pH 7.0, Fig. 2b) is similar to that of the COU spectrum. The maxima of the two peaks are at ~360 and 430 nm. The intensity of the transient peak at the lower wavelength is strongly influenced by the absorbance of 3-CCA in this wavelength region (Yamashita et al., 2012). The longer wavelength band here is much stronger ($\varepsilon_{430\ nm} \approx 3000$ mol^{-1} dm^3 cm^{-1}) than in the case COU. Our measured rate constant of the $^\bullet$OH reaction is 4.9×10^9 mol^{-1} dm^3 s^{-1}. This $k_{\bullet OH}$ is close to the values measured in other works, as an average of 5 determinations in Table 1 we obtain $5.64 \pm 0.78 \times 10^9$ mol^{-1} dm^3 s^{-1}.

9
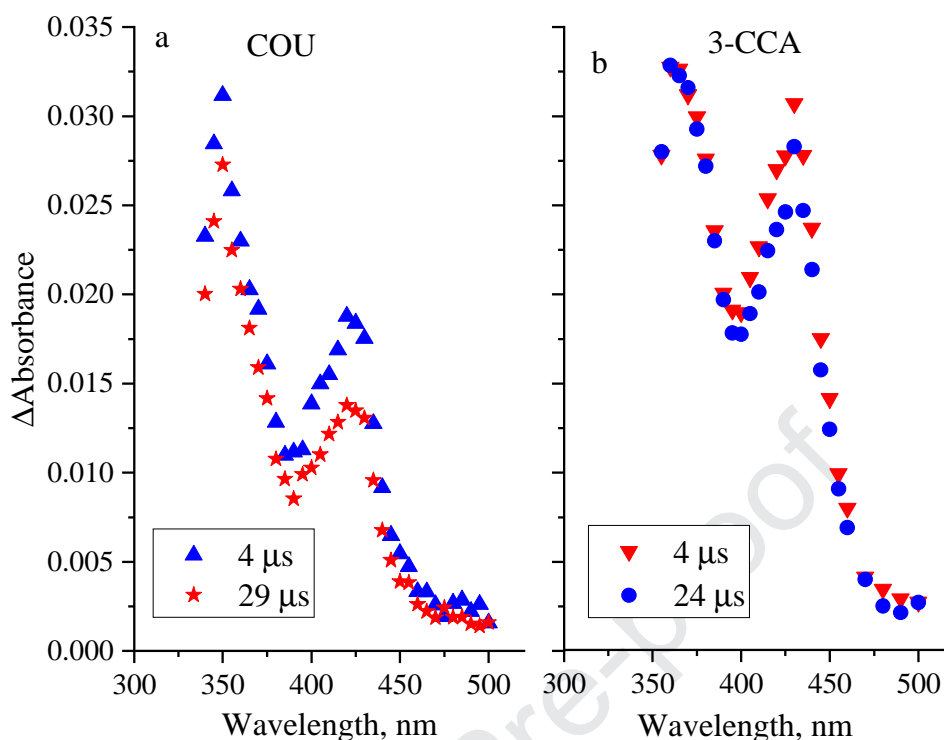
Figure 2. Transient absorption spectra observed in 2.0×10^{-4} mol dm^{-3} N$_2$O saturated COU (a) and 3-CCA (b) solutions, 1.0×10^{-2} mol dm^{-3} phosphate buffer (pH ~7), 20 Gy.

$^{\bullet}$OH is suggested to react with both molecules by addition to the electron rich aromatic ring (Singh et al., 2002; Yamashita et al., 2012). The reaction with the electron deficient pyranone ring is probably less important. The addition may take place at any carbon atoms of the aromatic ring, the wide absorption bands suggest the coexistence of several adduct isomers. The decay of the different adducts is expected to take place in radical-radical self-termination reactions. The absorption spectra just slightly change during the decay.
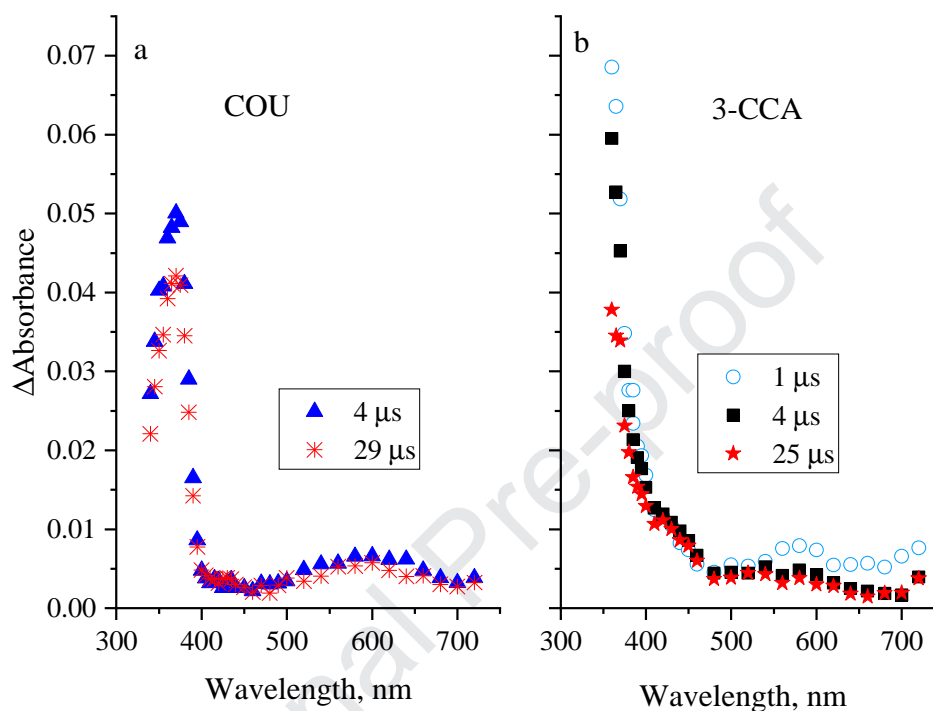
The reactions of the e$_{aq}^-$ were investigated at pH 8 in solutions saturated with N$_2$ for deoxygenation. The solutions contained t-BuOH in order to remove $^{\bullet}$OH in the reaction:

$^{\bullet}$OH + (CH$_3$)$_3$COH → H$_2$O + $^{\bullet}$CH$_2$(CH$_3$)$_2$COH
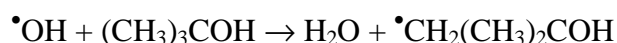
$$k = 6.0 \times 10^8 \text{ mol}^{-1} \text{ dm}^3 \text{ s}^{-1} \text{ (Buxton et al., 1988) (3)}$$
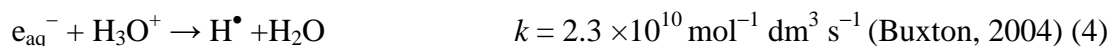
The absorption spectra for both molecules exhibit wide and weak bands between 500 and 700 nm, there are shoulders around 425 nm and strong bands at 360-370 nm (Fig. 3). The

10

latter bands reflects e_{aq}^{-} addition to the $>C=O$ group forming radical anion in the first step. This anion undergoes fast protonation giving a neutral radical $>C^{\bullet}\text{-}OH$ (Singh et al., 2002). The rate constants were determined by following the decay of the e_{aq}^{-} around the absorbance maximum at 720 nm. The timescale of the decay was 1 - 3 µs.
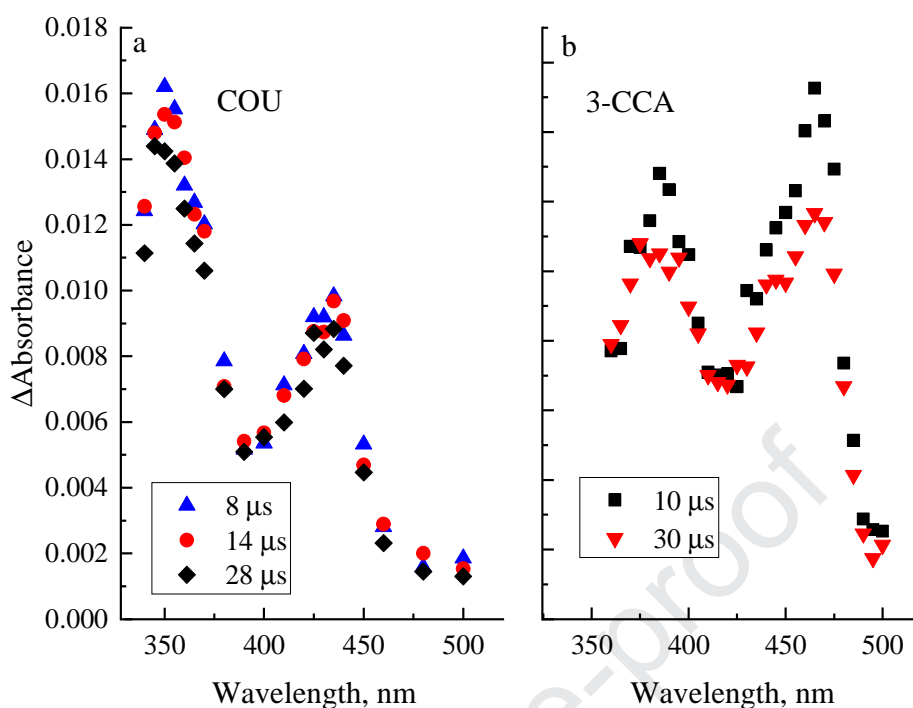

Figure 3. Transient absorption spectra observed in t-BuOH containing, N_2 saturated, 2.0×10^{-4} mol dm^{-3} COU (a) and 3-CCA (b) solutions at pH 8.0, 20 Gy.

In the acidic pH range e_{aq}^{-} transforms to $H^{\bullet}$:

$$e_{aq}^{-} + H_3O^{+} \rightarrow H^{\bullet} + H_2O \qquad k = 2.3 \times 10^{10}\,\text{mol}^{-1}\,\text{dm}^3\,\text{s}^{-1} \text{ (Buxton, 2004) (4)}$$
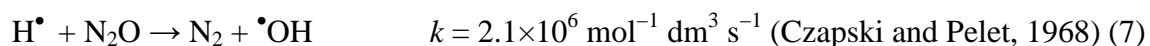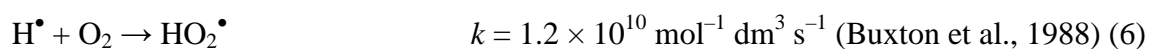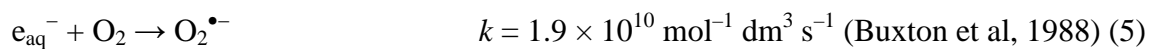
$H^{\bullet}$ reactions were investigated at pH 2.4. At this pH 3-CCA is mainly in the protonated form. COU and 3-CCA react with $H^{\bullet}$ with rate constants of 2.5×10^9 and 1.3×10^9 mol^{-1} dm^3 s^{-1}. The absorption spectra detected in $H^{\bullet}$ reaction to large extent are similar to the spectra measured in $^{\bullet}OH$ reaction: the maxima of the two peaks in $H^{\bullet}$ reaction are at 385 and 465 nm for COU and 360 and 430 nm for 3-CCA (Fig. 4). The similarity is not surprising, since the reductive $H^{\bullet}$ also adds to the double bonds similarly to the oxidative $^{\bullet}OH$, the distribution of the radical adducts also may show similarities.

11

Figure 4. Transient absorption spectra observed in t-BuOH containing, N_2 saturated, 2.0×10^{-5} mol dm^{-3} COU (a) and 3-CCA (b) solutions at pH 2.4, 20 Gy.
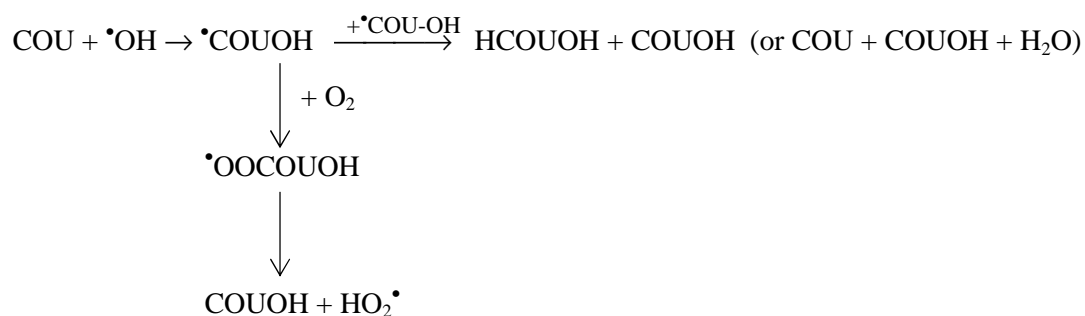
3.2. Gamma-radiolysis

Using gamma-radiolysis the aim was to investigate the possible role of e_{aq}^-, H$^\bullet$ and dissolved O_2 in fluorescent hydroxylated products formation. The radiolysis measurements were performed in O_2 saturated, N_2O saturated, and in O_2-free and t-BuOH containing solutions. Both O_2 and N_2O react with e_{aq}^- (3 and 5) and H$^\bullet$ (6 and 7):

$$e_{aq}^- + O_2 \rightarrow O_2^{\bullet-} \qquad\qquad k = 1.9 \times 10^{10} \text{ mol}^{-1} \text{ dm}^3 \text{ s}^{-1} \text{ (Buxton et al, 1988) (5)}$$

$$H^\bullet + O_2 \rightarrow HO_2^\bullet \qquad\qquad k = 1.2 \times 10^{10} \text{ mol}^{-1} \text{ dm}^3 \text{ s}^{-1} \text{ (Buxton et al., 1988) (6)}$$

$$H^\bullet + N_2O \rightarrow N_2 + {}^\bullet OH \qquad k = 2.1 \times 10^6 \text{ mol}^{-1} \text{ dm}^3 \text{ s}^{-1} \text{ (Czapski and Pelet, 1968) (7)}$$

In N_2O and O_2 saturated solutions the transformation of both COU and 3-CCA is initiated by the reaction with $^\bullet$OH. N_2O transforms e_{aq}^- to $^\bullet$OH, therefore, the $^\bullet$OH formation rate is two times higher in N_2O saturated solution than in O_2 saturated one. Another significant difference between the N_2O and O_2 saturated solution is the possibility for the formation of

12

peroxyl type radicals, which generally has an important role in the transformation of parent compound and formation of hydroxylated intermediates. Louit et al., (2005) proposed two different ways for the formation of hydroxylated products from COU. The carbon centered radical formed by the addition of $^\bullet$OH to aromatic ring may evolve by dismutation reaction toward hydroxycoumarins and COU. In the presence of O_2 via formation of peroxyl radical and $HO_2^\bullet$ elimination, hydroxycoumarins form in a unimolecular reaction and the backward reaction (COU formation) is inhibited. Similar ways can be proposed for $^\bullet$OH initiated transformation of 3-CCA and formation of its hydroxylated products.
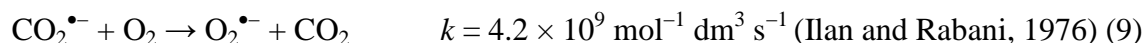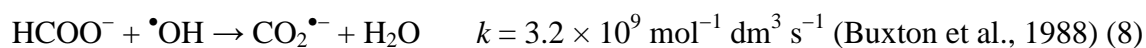
$$COU + {}^\bullet OH \rightarrow {}^\bullet COUOH \xrightarrow{+ {}^\bullet COU\text{-}OH} HCOUOH + COUOH \ (or \ COU + COUOH + H_2O)$$

$$\downarrow + O_2$$

$${}^\bullet OOCOUOH$$

$$\downarrow$$

$$COUOH + HO_2^\bullet$$

Although, the formation rate of $^\bullet$OH is two times higher in the presence of N_2O, there is no significant difference between the transformation rates of COU and formation rates of 7-HO-COU in solution saturated with O_2 or N_2O. Similar observations were made in the case of 3-CCA (Fig. 5). In N_2 saturated, t-BuOH containing solution at pH 2.1 the transformation of COU is slightly slower, while that of 3-CCA is slightly faster than in O_2 saturated solutions (Fig. 5a and c). At this pH, e_{aq}^- is transformed to $H^\bullet$ via protonation. Thus, the transformation of both COU and 3-CCA is initiated by $H^\bullet$. Under these conditions, formation of 7-HO-COU and 7-HO-3-CCA was not detected (Fig. 5b and d). The radiolysis results obtained under various experimental conditions show that, the formation of both 7-HO-COU and 7-HO-3-CCA requires $^\bullet$OH-initiated transformation of COU and 3-CCA and the yield of the hydroxylated products is highly enhanced by the presence of dissolved O_2, which opens up a new way of the formation via peroxyl type radicals.
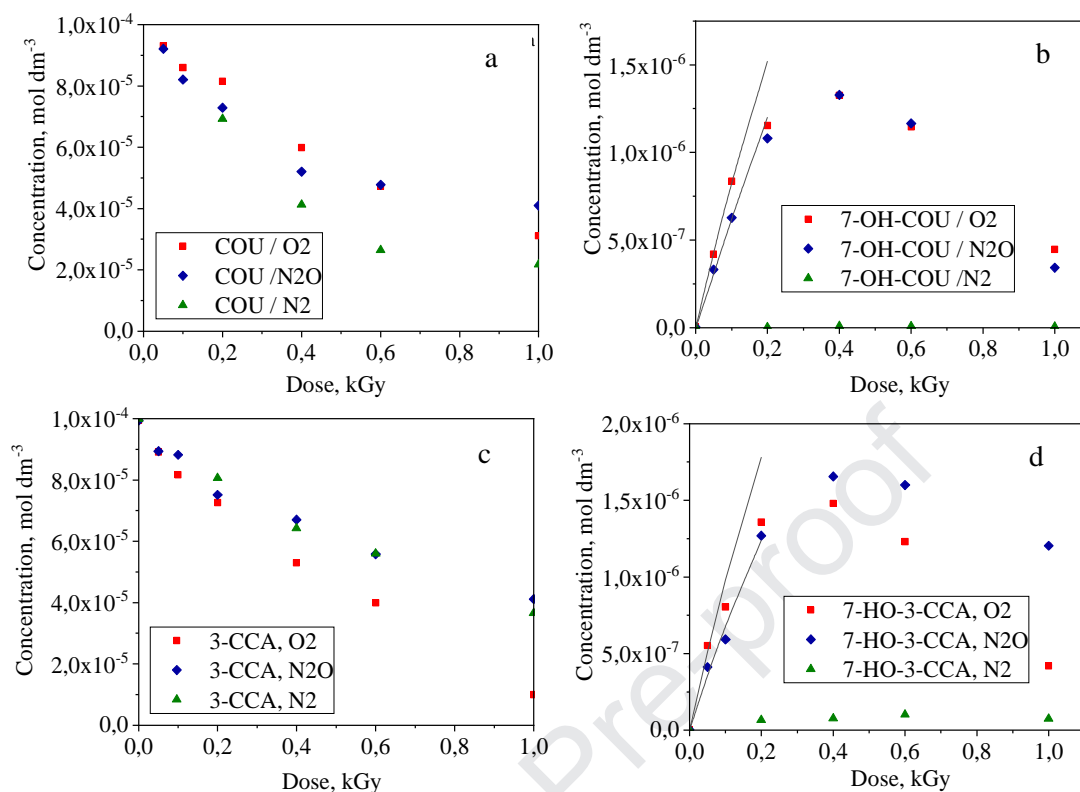
Figure 5. The concentration of COU (a), 7-HO-COU (b), 3-CCA (c) and 7-HO-3-CCA (d) versus absorbed dose at pH 2.1

■: O_2 saturated solution; ◆: N_2O saturated solution; ▲: O_2- free, t-BuOH (5 v/v%) containing solution

The $O_2^{\bullet-}/HO_2^{\bullet}$ pair (pK_a 4.8) is rather inactive in reaction with most of aromatic molecules (Yamashita et al., 2012; Kozmér et al., 2014). In this work the reaction with $O_2^{\bullet-}$ were investigated in 1.0×10^{-4} mol dm^{-3} NaCOOH containing COU solution (pH 8). Under these circumstances $^{\bullet}$OH was converted into $O_2^{\bullet-}$:

$$HCOO^- + {^{\bullet}OH} \rightarrow CO_2^{\bullet-} + H_2O \qquad k = 3.2 \times 10^9 \text{ mol}^{-1} \text{ dm}^3 \text{ s}^{-1} \text{ (Buxton et al., 1988) (8)}$$
$$CO_2^{\bullet-} + O_2 \rightarrow O_2^{\bullet-} + CO_2 \qquad k = 4.2 \times 10^9 \text{ mol}^{-1} \text{ dm}^3 \text{ s}^{-1} \text{ (Ilan and Rabani, 1976) (9)}$$

Transformation of COU was not observed in this case, showing that $O_2^{\bullet-}$ (and most likely its protonated form $HO_2^{\bullet}$ also) has no role in the transformation of COU and formation of fluorescent hydroxylated product.

14

The formation rates of $^{\bullet}$OH were calculated from the dose rate (in these experiments 1.48 Gy min^{-1}) and radiation chemical yields (*G* value) of the $^{\bullet}$OH formation (0.28 µmol J^{-1} in O$_2$ saturated and O$_2$-free and 0.54 µmol J^{-1} in N$_2$O saturated solutions). The $^{\bullet}$OH formation values calculated by this way were 6.9×10^{-9} mol dm^{-3} s^{-1} and 1.33×10^{-8} mol dm^{-3} s^{-1}. Radiation chemical yields of the formation of 7-HO-COU and 7-HO-3-CCA were determined from the slope of the plots of concentration versus dose in N$_2$O saturated (O$_2$-free without t-BuOH), and O$_2$ saturated solutions (pH = 6.5). As the curves with maxima on Fig. 5b and 5d show the formed fluorescing products undergo secondary decomposition even at low doses. This secondary decomposition affects also the determination of the initial formation rate. A correction was applied using the method of Albarran and Schuler (2003). In Fig. 5b and 5d the solid curves show the calculated correction curves. It should be mentioned that the value obtained for 7-HO-COU formation in O$_2$ saturated solution (9.4×10^{-9} mol J^{-1}) is lower than this value determined by Ashawa et al. (1979) (1.05×10^{-8} mol J^{-1} at 1 Gy min^{-1}dose rate) or Louit et al. (2005) (1.4×10^{-8} mol J^{-1} at 1.9 Gy min^{-1}) in aerated solution. Similarly, the value determined by Collins et al. (1994) for 7-HO-3-CCA (1.27×10^{-8} mol J^{-1} at 4 Gy min^{-1}) is also higher than that was determined in this work (8.0×10^{-9} mol J^{-1}).

The relative production yields of the hydroxylated products (formation rate of 7-HO-COU or 7-HO-3-CCA divided by the formation rate of $^{\bullet}$OH) were found to be significantly higher in the presence of dissolved O$_2$ confirming the important role of peroxyl radical in their formation. This is in agreement with observations reported previously (Louit et al (2005). However, our value determined in O$_2$ saturated solution (0.034) is lower than that reported previously in aerated solutions 0.044 (Manevich et al, 1997) and 0.047 (Yamashita el al. 2012) for 7-HO-3-CCA). The efficiency of fluorescing product formation depends on several factors, e.g., dose rate, oxygen concentration, CUO and 3-CCA concentration. To find the reason of the differences in the efficiency values determined by us and published in the literature needs further investigations.
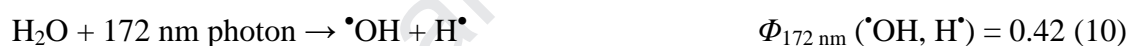
Table 2. Transformation rates (r_0), radiation chemical yields (G) and relative production yield of the hydroxylated products ($\mathbf{r_0}^{\textbf{7-HO-COU}} / \mathbf{r_0}^{\bullet\textbf{OH}} \times 100$ or $\mathbf{r_0}^{\textbf{7-HO-3-CCA}} / \mathbf{r_0}^{\bullet\textbf{OH}} \times 100$)

	7-HO-COU			7-HO-3-CCA		
	$\mathbf{r_0}^{\textbf{7-HO-COU}}$ ($\times 10^{-10}$ mol dm^{-3} s^{-1})	$\mathbf{G}^{\textbf{7-HO-COU}}$ ($\times 10^{-9}$ mol J^{-1})	$\mathbf{r_0}^{\textbf{7-HO-COU}}/\textbf{ro}^{\bullet\textbf{OH}}$	$\mathbf{r_0}^{\textbf{7-HO-3-CCA}}$ ($\times 10^{-10}$ mol dm^{-3} s^{-1})	$\mathbf{G}^{\textbf{7-HO-3-CCA}}$ ($\times 10^{-9}$ mol J^{-1})	$\mathbf{r_0}^{\textbf{7-HO-3-CCA}}/\textbf{ro}^{\bullet\textbf{OH}}$
N$_2$	0.65	2.6	0.009	0.93	3.8	0.014
N$_2$O	1.9	7.6	0.014	2.7	11.0	0.02
O$_2$	2.3	9.4	0.034	2.0	8.4	0.03

3.3. VUV photolysis

In 172 nm VUV photolysis, homolytic dissociation of water molecules produces $^\bullet$OH and H$^\bullet$ reactive intermediates with a quantum yield of 0.42 (Heit et al., 1998). Although ionization of water also takes place, the role of e_{aq}^- initiated reactions is generally neglected because of the low quantum yield (0.045) of e_{aq}^- formation.

$$\text{H}_2\text{O} + 172 \text{ nm photon} \rightarrow {}^\bullet\text{OH} + \text{H}^\bullet \qquad \Phi_{172 \text{ nm}} ({}^\bullet\text{OH, H}^\bullet) = 0.42 \quad (10)$$

$$\text{H}_2\text{O} + 172 \text{ nm photon} \rightarrow \text{H}^+ + e_{aq}^- + {}^\bullet\text{OH} \qquad \Phi_{172 \text{ nm}} (e_{aq}^-) = 0.045 \quad (11)$$

Due to the high molar absorbance of water at 172 nm (550 cm^{-1}, Weeks et al., 1963), these VUV photons are absorbed in a very thin, 0.035 mm (Al-Gharabli et al., 2016) water layer, called 'photoreaction zone'. Within this zone, the primarily formed radicals ($^\bullet$OH and H$^\bullet$) may react with organic substances. Since the concentration of these radicals is very high in the photoreaction zone, their recombination with each other (H$^\bullet$ + H$^\bullet$, H$^\bullet$ + $^\bullet$OH and $^\bullet$OH + $^\bullet$OH) can occur with high probability. These radical-radical reactions have rate constants in the 5×10^9 - 8×10^9 mol^{-1} dm^3 s^{-1} range (Buxton et al., 1988).
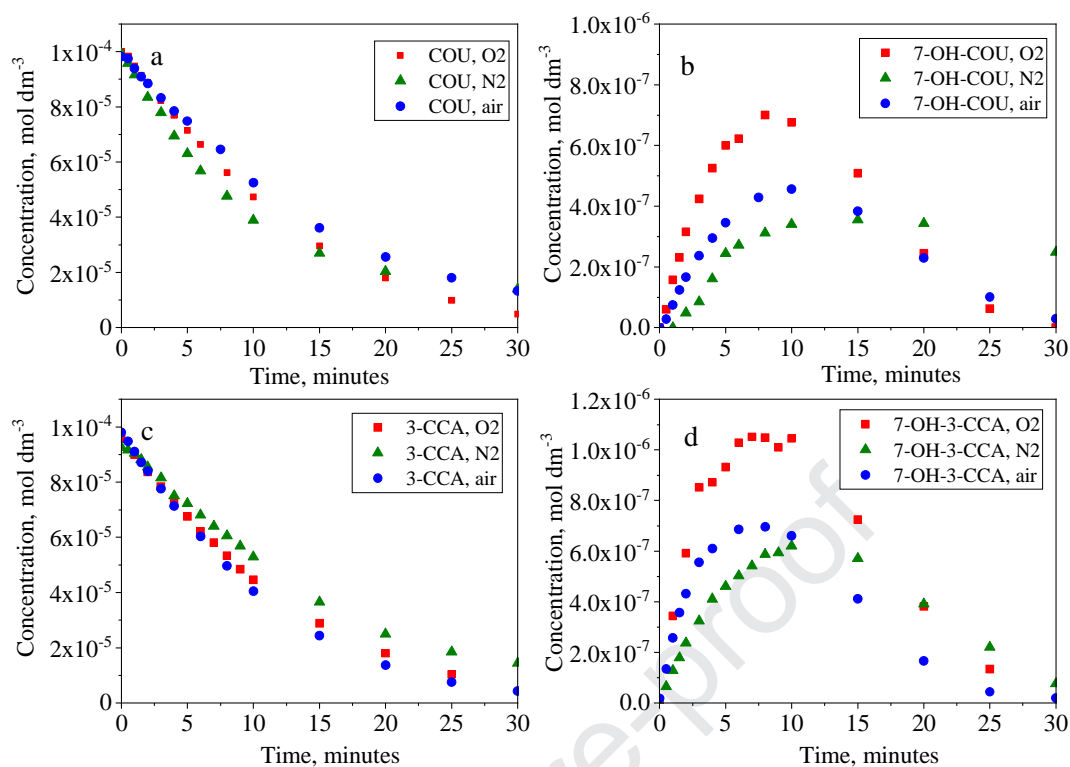
Figure 6. Concentration of COU (a), 7-HO-COU (b), 3-CCA(c) and 7-HO-3-CCA (d) versus time of VUV radiation

■: O_2 saturated solution; ●: air saturated solution; ▲: O_2- free solution

Table 3. Effect of dissolved O_2 on the initial transformation rate of COU, 3-CCA and the formation rate of 7-HO-COU and 7-HO-3-CCA in the case of VUV photolysis

	Transformation and formation rates			
	COU ($\times 10^{-7}$ mol dm^{-3} s^{-1})	7-HO-COU ($\times 10^{-9}$ mol dm^{-3} s^{-1})	3-CCA ($\times 10^{-7}$ mol dm^{-3} s^{-1})	7-HO-3-CCA ($\times 10^{-9}$ mol dm^{-3} s^{-1})
N_2	1.23	1.33	1.03	1.95
Air	0.87	1.43	1.21	3.78
O_2	1.01	2.68	0.97	4.67

The effects of dissolved O_2 and the effective $^\bullet$OH radical scavengers, MeOH and t-BuOH were investigated. Although O_2 opens up new pathways for transformation of carbon centred radicals and generally enhances the transformation rate of organic substances, its effect on the initial transformation rates was not observable in the VUV photolysis of COU and 3-CCA (Fig. 6 and Table 3). The reason can be that, O_2 reacts with H$^\bullet$ (6), thus eliminates

17

one of the reactive species from the radical set, compensating the positive effect of peroxyl radicals by this way.

Although the dissolved O_2 has not significant effect on the transformation rates of COU and 3-CCA, the formation rate of both 7-HO-COU and 7-HO-3-CCA was more than two times higher in O_2 saturated solution ($c(O_2) = 1.25 \times 10^{-5}$ mol dm^{-3}) than in O_2-free one (Fig. 6 and Table 3). The radiolysis results proved, that the formation of hydroxylated products requires $^{\bullet}OH$, while dissolved O_2 enhances that via formation of peroxyl radical. In the case of VUV photolysis of COU, in air ($c(O_2) = 2.5 \times 10^{-4}$ mol dm^{-3}) saturated solution the formation rate of 7-HO-COU is slightly, while in the case of 3-CCA significantly higher than under O_2-free conditions, but lower than in O_2 saturated solutions. The high radical concentration in the VUV light irradiated very thin photoreaction zone causes O_2 depletion (Heit et al., 1998). Thus, using air, the positive effect of dissolved O_2 is probably strongly limited by its lower concentration. Moreover, degree of O_2 deficiency depends on the reaction rates and on the way of the further transformation of carbon centred and peroxyl radicals.

MeOH or t-BuOH, were added to the VUV irradiated solutions for further investigation of $^{\bullet}OH$ based reactions. The ratios of COU/3-CCA:MeOH/t-BuOH were 1:1; 1:10; 1:50 and 1:100. Fig. 7 shows the rate of COU/3-CCA degradation and that of 7-OH-COU/7-OH-3-CCA formation as a function of relative $^{\bullet}OH$ scavenging capacity (RSC$_{\bullet OH}$):

$$RSC_{\bullet OH} = 1 - c_{\,COU/3\text{-}CCA} \times k_{\,COU/3\text{-}CCA.} \, / \, (c_{\,COU/3\text{-}CCA} \times k_{\,COU/3\text{-}CCA} + c_{\,cav.} \times k_{\,scav.})$$

where c_{COU} and $c_{3\text{-}CCA}$ are the COU and 3-CCA initial concentrations, and k_{COU} and $k_{3\text{-}CCA}$ are the rate constants of reactions with $^{\bullet}OH$. The rate constant of $^{\bullet}OH$ reactions with COU and 3-CCA were taken as 6.9×10^9 and 4.9×10^9 mol^{-1} dm^3 s^{-1}, respectively (Table 1). The values for the scavengers, MeOH, t-BuOH (k(MeOH + $^{\bullet}OH$) = 9.7×10^8 mol^{-1} dm^3 s^{-1} and k(t-BuOH) + $^{\bullet}OH$) = 6.0×10^8 mol dm^{-3} s^{-1} (Buxton et. al, 1988)) were collected from the NDRL/NIST compilation. When the RSC$_{\bullet OH}$ is 0 only COU or 3-CCA is present, and there is no scavenger in the system. RSC$_{\bullet OH}$ value shows the ratios of the $^{\bullet}OH$ amounts, which are scavenged by MeOH or t-BuOH relative that of COU or 3-CCA, at the given concentrations.

Addition of $^{\bullet}OH$ scavengers decreases the transformation rates of COU and 3-CCA (Fig. 7). At the highest MeOH and t-BuOH concentrations the majority of $^{\bullet}OH$ reacts with alcohols but maximum 10% of H$^{\bullet}$ are scavenged (k(MeOH + H$^{\bullet}$) = 2.6×10^6 mol^{-1} dm^3 s^{-1} and k(t-BuOH) + H$^{\bullet}$) = 2.3×10^5 mol^{-1} dm^3 s^{-1} (Buxton et al., 1988)) in O_2-free solutions. In this case, the transformation rate of COU and 3-CCA decreased by 66 - 73% in O_2 saturated

18

solutions but only by 35 - 46% in O_2-free solutions, respectively. In the latter case the scavenging effect is less pronounced, since both COU and 3-CCA are able to react with $H^\bullet$ (Table 1).
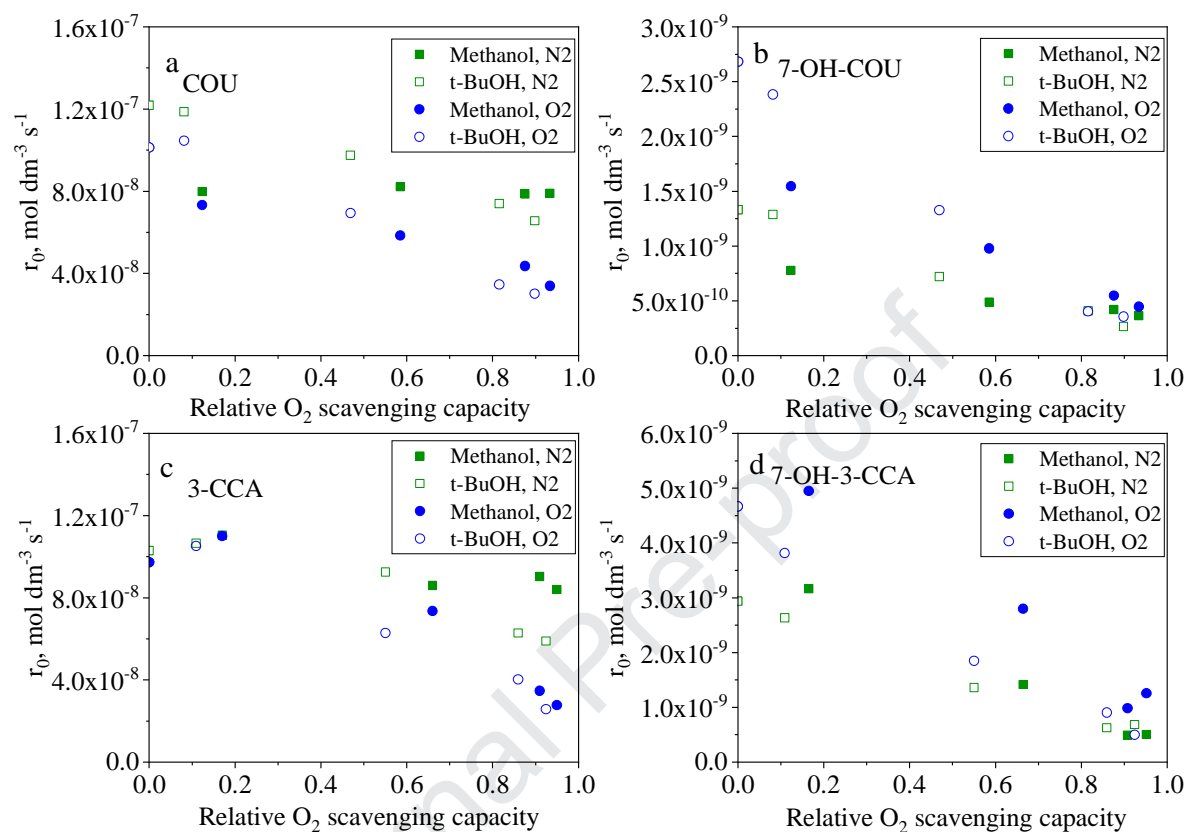
Figure 7. Effect of MeOH and t-BuOH on the transformation rate of COU (a) and 3-CCA (c) and formation rate of 7-HO-COU (b) and 7-HO-3-CCA (d) in O_2-free and O_2 saturated VUV irradiated solutions

■: MeOH, O_2-free solution; □: t-BuOH; O_2-free solution; ●: MeOH; O_2 saturated solution; ○: t-BuOH; O_2 saturated solution

The yield of hydroxylated product is about two times higher in the presence of O_2 in both cases. Moreover, the yield of 7-HO-3-CCA formation from 3-CCA is about two times higher than that of 7-HO-COU from COU (Fig. 7 and Table 2); the rate constant of COU reaction with $^\bullet OH$ exceeds that of 3-CCA (Table 1).

The formation of 7-HO-COU is more sensitive to the decrease of $^\bullet OH$ concentration than the transformation of COU. When about 10% of $^\bullet OH$ reacts with MeOH, the transformation rate of COU does not decrease significantly, while formation rate of 7-HO-COU decreases by

almost 50% (Fig. 7). Further increase of $RSC_{\bullet OH}$ value causes a less intensive effect. The behaviour of 3-CCA is a little bit different from that of COU. Addition of MeOH or t-BuOH at 1:1 ratio has no negative effect, but at higher concentration of additives the inhibition is well manifested (Fig. 7).

In the case of VUV photolysis the formation rate of $^\bullet OH$ can be calculated from the photon flux (3.0×10^{-6} mol_{photon} s^{-1}) and quantum yield of $^\bullet OH$ formation via absorption at 172 nm light (0.42) and the volume of radiated solution (0.50 dm^{-3}). The $^\bullet OH$ formation rate calculated by this way is 2.52×10^{-6} $mol_{\bullet OH}$ dm^{-3} s^{-1}. Using the relative production yield of the hydroxylated products obtained from radiolysis and the formation rate of 7-HO-CUO and 7-HO-3-CCA determined in O_2-free VUV irradiated solutions, the formation rate of $^\bullet OH$ is 1.42×10^{-7} mol dm^{-3} s^{-1} for 7-HO-COU and 1.61×10^{-7} mol dm^{-3} s^{-1} for 7-HO-3-CCA. These values are much lower than those calculated from the photon flux. One possible explanation is the extreme inhomogeneity of the VUV irradiated solution, where the concentration of $^\bullet OH$ and $H^\bullet$ in the VUV irradiated 0.035 mm thin photoreaction zone is very high, thus $^\bullet OH$ decay in radical-radical ($^\bullet OH + {}^\bullet OH$, $^\bullet OH + H^\bullet$) reactions is favoured. Consequently, a high percentage of $^\bullet OH$ disappears from the system without the formation of hydroxylated product. The formation rates of $^\bullet OH$ calculated by the same way in O_2 saturated solution are even lower for 7-HO-COU (8.1×10^{-8} mol dm^{-3} s^{-1}), while a little bit higher in the case of 7-HO-3-CCA (1.64×10^{-7} mol dm^{-3} s^{-1}). The inhomogeneity of VUV irradiated systems is manifested not only in the radical concentration, but also in the concentration of dissolved O_2 versus the distance from the wall of the light source (Al-Gharabi et al., 2016).

3.4. Heterogenous photocatalysis

In the case of heterogeneous photocatalysis $^\bullet OH$ is the main reactive species. The photon absorption results in charge separation in the photocatalyst: an electron in the conduction band (e_{cb}^-), and a hole (h_{vb}^+) are created. Dissolved O_2 generally has a crucial role as e_{cb}^- scavenger, which is needed to retard the fast recombination of h_{vb}^+ and e_{cb}^-. On the surface of TiO_2 e_{cb}^- can transform to $O_2^{\bullet-}$ via reaction with adsorbed O_2. Further transformation of $O_2^{\bullet-}$ via H_2O_2 results in $^\bullet OH$ (Nosaka et al., 2014). Another possible way of $^\bullet OH$ formation is the reaction of OH^-/H_2O with h_{vb}^+. The transformation of organic substances can take place *via* direct charge transfer and/or *via* reaction with $^\bullet OH$ on the surface ($^\bullet OH_{surf}$) or in the bulk phase ($^\bullet OH_{bulk}$). The contribution of these pathways to the

transformation of target organic substances depends strongly on the properties of the photocatalyst, the model compound and the interaction between them.

The main difference in the behaviour of COU and 3-CCA in photocatalytic experiments is their interaction with TiO_2 surface: COU is poorly adsorbed (the adsorbed amount is not measurable), while 3-CCA is well adsorbed (30% of 3-CCA adsorbed at 1.0×10^{-4} mol dm^{-3} initial concentration in 1.0 g dm^{-3} TiO_2 suspension independently of the presence of O_2) because of the strong interaction between the carboxyl group and surficial hydroxyl groups of TiO_2 ($\equiv$Ti-OH).

Table 4. Effect of dissolved O_2 on the initial transformation rates of COU, 3-CCA and the formation rates of 7-HO-COU and 7-HO-3-CCA in the case of heterogeneous photocatalysis

	Transformation and formation rates			
	COU ($\times 10^{-7}$ mol dm^{-3} s^{-1})	**7-HO-COU** ($\times 10^{-9}$ mol dm^{-3} s^{-1})	**3-CCA** ($\times 10^{-7}$ mol dm^{-3} s^{-1})	**7-HO-3-CCA** ($\times 10^{-9}$ mol dm^{-3} s^{-1})
N₂	0.06	-	0.81	-
Air	1.18	3.50	1.38	3.92
O₂	1.19	5.15	1.75	5.21

At first the effect of dissolved O_2 was investigated. In O_2-free suspension the transformation rate of COU was negligible, while the transformation rate of 3-CCA was about half of that determined in O_2 containing suspensions (Table 3). This suggests that, there is a significant contribution of direct charge transfer to the transformation of 3-CCA. Because of the strong interaction of 3-CCA with $\equiv$Ti-OH groups and the high rate constants of its reaction with e_{aq}^-, 3-CCA can behave as e_{cb}^- scavenger, taking over the role of O_2. In N_2 purged suspension there are no possibilities for peroxyl radical or $^{\bullet}$OH formation via $O_2^{\bullet-}$/H_2O_2. The formation of $^{\bullet}$OH can take place exclusively from OH$^-$(H_2O) via reaction with h_{vb}^+. The formation of 7-HO-3-CCA was not observed, which indicates that, the role (and most probably the formation) of $^{\bullet}$OH is negligible in this case. The transformation of 3-CCA happens via direct charge transfer, which does not result in hydroxylated products.

Although there was no difference between the transformation rates of COU in O_2 saturated and aerated suspensions ($r_0^{COU}(O_2)/r_0^{COU}(air) = 1.01$), the formation rate of 7-HO-COU was 50% higher in the O_2 saturated one ($r_0^{7-HO-COU}(O_2)/r_0^{7-HO-COU}(air) = 1.47$). The ratio of 3-CCA transformation rates ($r_0^{3-CCA}(O_2)/r_0^{3-CCA}(air) = 1.27$) agreed with the ratio of formation rates of the hydroxylated product ($r_0^{7-HO-3-CCA}(O_2)/r_0^{7-HO-3-CCA}(air) = 1.33$). Probably

21

the COU transformation happens mainly via reaction with $^{\bullet}OH_{bulk}$, because COU cannot successfully compete for adsorption sites with O_2 or H_2O_2. At the same time, in the transformation of well adsorbed 3-CCA the $^{\bullet}OH_{surf}$ can also have important role. Moreover, the recombination of $^{\bullet}OH$, formed on the surface of TiO_2, is better inhibited by 3-CCA than by COU. This may be the reason why the transformation rate of 3-CCA is higher, while its rate constant of reaction with $^{\bullet}OH$ is lower than that of COU (Table 1).
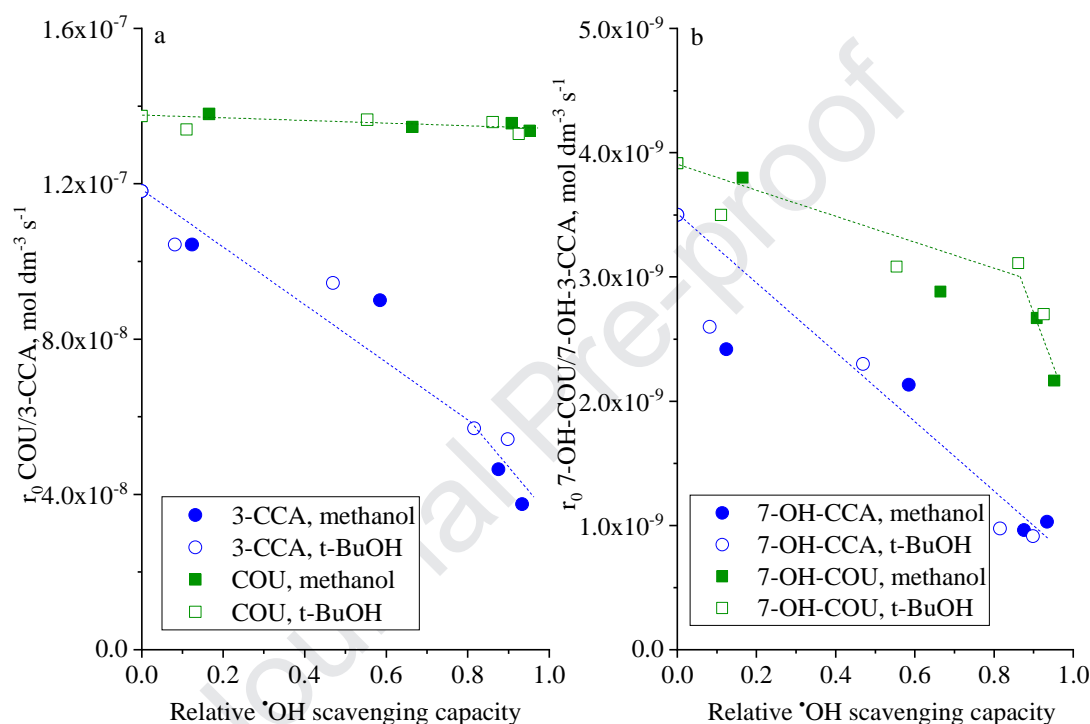
Figure 8. Rate of COU and 3-CCA (a) degradation and hydroxylated product formation (b) as a function of the relative scavenging capacity of MeOH and t-BuOH in heterogeneous photocatalysis

Figure 8. shows the effect of MeOH and t-BuOH on the transformation rate of COU and 3-CCA and on the formation rate of hydroxylated products in aerated suspensions. Both radical scavengers adsorbed poorly on the TiO_2 surface. When the degradation of both COU and the scavenger occurs independently and no preferred adsorption on the surface takes place a linear decrease of degradation rate with the RSC is expected. Although, the transformation rate of COU decreases linearly, there is a breakpoint at 0.6 scavenging capacity. Above this $RSC_{\bullet OH}$ value, the inhibition gets higher. Most probably, at relatively high concentration of

radical scavengers they can react not only with $^\bullet OH_{bulk}$ but also with $^\bullet OH_{surf}$, thus their scavenging effect is increased.

The same $^\bullet OH$ scavengers have no observable effect on the transformation rate of 3-CCA (Fig. 8a). This also proves the crucial role of adsorption. Poorly adsorbed radical scavengers are not able to compete successfully with the well-adsorbed 3-CCA for $^\bullet OH_{surf}$. At the same time the formation of hydroxylated product is inhibited. The breaking point is at 0.80 RSC value: at lower MeOH/t-BuOH concentrations the formation rate of 7-HO-3-CCA is only slightly inhibited, probably because both MeOH and t-BuOH react mainly with $^\bullet OH_{bulk}$. Further increase of the scavenger concentrations cause a more advanced inhibition. The explanation can be the same as in the case COU: the increase of the poorly absorbed radical scavenger's concentration makes their reaction with $^\bullet OH_{surf}$ possible.

Using the production yield of the hydroxylated products obtained from radiolysis and the formation rate of 7-HO-CUO and 7-HO-3-CCA determined in O_2-saturated TiO_2 suspensions, the formation rate of $^\bullet OH$ was determined. The obtained values are in good agreement with each other: 1.56×10^{-7} mol dm^{-3} s^{-1} for 7-HO-COU and 1.80×10^{-7} mol dm^{-3} s^{-1} for 7-HO-3-CCA. Assuming that, TiO_2 suspension completely absorbs the emitted photons, the calculated quantum yield for the $^\bullet OH$ formation is about 0.006 (0.0054 for 7-HO-COU and 0.0062 for 7-HO-3-CCA). Therefore, on average the 0.6% of the absorbed photons are converted to $^\bullet OH$. The quantum yield of $^\bullet OH$ production during TiO_2 photocatalysis was estimated to be lower (~10^{-4}) by a method based on the terephthalic acid (Ishibashi et al., 2000), while using methanol higher value (0.02 – 0.08) was reported (Wang et al., 2001).

Summary

The transformation of COU, 3-CCA and formation of their fluorescent hydroxylated products (7-HO-COU and 7-HO-3-CCA) were investigated. Reaction rate constants of both compounds with $^\bullet HO$, $H^\bullet$ and e_{aq}^- were determined. The results of gamma-radiolysis proved that the formation of fluorescent products takes place only via reaction with $^\bullet OH$ and the rate is enhanced by the presence of O_2. The ratio of the $^\bullet OH$ formation rate and the formation rate of fluorescent products were determined in O_2-free, O_2 and N_2O saturated solutions.

In the case of VUV photolysis, the presence of O_2 has no significant effect on the transformation rate of parent compounds, while formation rates of both 7-HO-COU and 7-HO-3-CCA were more than two times higher in O_2 saturated than in O_2-free solution. The effect of MeOH and t-BuOH as $^\bullet OH$ scavengers showed, that formation rate of hydroxylated

products is more sensitive to the decrease of $^\bullet$OH concentration than the transformation rate of parent compounds, mainly in the presence of O_2. The formation rate of $^\bullet$OH was calculated from the photon flux and quantum yield of $^\bullet$OH formation via absorption at 172 nm light. It was compared to that determined by the relative production yield of the hydroxylated products obtained from radiolysis and the formation rate of 7-HO-CUO and 7-HO-3-CCA determined in O_2-free VUV irradiated solutions. The latest values were much lower, which can be explained partly by the extreme inhomogeneity of VUV irradiated solution.

Using heterogeneous photocatalysis, the quantum yield of the $^\bullet$OH formation (0.006) was determined using the data obtained from radiolysis and formation rate of 7-HO-3-CCA and 7-HO-COU. There was no difference between the yield of the 7-HO-3-CCA formed from the well adsorbed 3-CCA and 7-HO-COU, formed from the poorly adsorbed COU. However, the dominant role of $^\bullet$OH is evident, the preferred adsorption of 3-CCA did not let the manifestation of the inhibition effect of MeOH and t-BuOH on its transformation rate. At the same time, the formation rate of 7-HO-3-CCA linearly decreased with the $^\bullet$OH scavenging capacity of both MeOH and t-BuOH. Our results suggested, that the transformation of the COU is controlled by its reaction with $^\bullet$OH$_{bulk}$ while in the case of 3-CCA, the reaction with $^\bullet$OH$_{surf}$ is the dominant. Adsorption has to be taken into consideration when the effect of $^\bullet$OH scavengers is evaluated.

References

Al-Gharabli S, Engeßer P, Gera D, Klein S, Oppenländer T. 2016. Engineering of a highly efficient Xe_2^*-excilamp (xenon excimer lamp, λ_{max} = 172 nm, η = 40%) and qualitative comparison to a low-pressure mercury lamp (LP-Hg, λ = 185/254 nm) for water purification. Chemosphere 144, 811-815.

Albarran G., Schuler, R.H., 2003. Concerted effects in the reaction of $^\bullet$OH radicals with aromatics: radiolytic oxidation of salicylic acid. Radiat. Phys. Chem. 67, 279-285.

Arany, E., Szabó, R.K., Apáti, L., Alapi, T., Ilisz, I., Mazellier, P., Dombi, A., Gajda-Schrantz, K., 2013. Degradation of naproxen by UV, VUV photolysis and their combination. J. Hazard. Mater. 262, 151–157.

Ashawa, S.C., Kini, U.R., Madhvanath, U., 1979. The aqueous coumarin system as a low range chemical dosimeter. Appl. Radiat. Isot. 30, 7–10.

Buxton, G., Greenstock, C.L., Helman, W.P., Ross, A.B., 1988. Critical review of rate constants for reactions of hydrated electrons, hydrogen atoms and hydroxyl radicals ($^\bullet$OH/O$^-$) in aqueous solution. J. Phys. Chem. Ref. Data 17, 513–886.

Buxton, G.V., 2004. The radiation chemistry of liquid water: principles and applications. In: Mozumder A, Hatano Y (eds) Charged particle and photon interaction with matter, Marcel Dekker, New York, pp. 331–365.

Czapski, G., Peled, E., 1968. On the pH-dependence of G reducing in the radiation chemistry of aqueous solutions. Isr. J. Chem. 6, 421–436.

Černigoj, U., Štangar, U.L., Trebše, P., Sarakha, M., 2009. Determination of catalytic properties of TiO$_2$ coatings using aqueous solution of coumarin: Standardization efforts. J. Photochem. Photobiol. A 201, 142–150.

Collins, A.K., Makrigiorgos, G.M., Svensson, G.K., 1994. Coumarin chemical dosimeter for radiation therapy. Med. Phys 21, 1741–1747.

Czili, H., Horváth, A. 2008. Applicability of coumarin for detecting and measuring hydroxyl radicals generated by photoexcitation of TiO2 nanoparticles Appl. Catal., B 81, 295–302.

Földiák, G., Hargittai, P., Kaszanyiczki, L., Wojnárovits, L., 1988. A computer controlled pulse radiolysis laboratory. J. Radioanal. Nucl. Chem. 125, 19–28.

Gopakumar, K., Kini, U.R., Ashawa, S.C., Bhandari, N.S., Krishnan, G.U., Krishnan, D., 1977. Gamma irradiation of coumarin in aqueous solution. Radiat. Effects 32, 199–203.

Hatchard, C.G., Parker, C.A. 1956. A new sensitive chemical actinometer. II. Potassium ferrioxalate as a standard chemical actinometer. Proc. Royal Soc. A 235, 518-536.

Heit, G., Neuner, A., Saugy, P.-Y., Braun, A.M., 1998. Vacuum-UV (172 nm) actinometry. The quantum yield of the photolysis of water. J. Phys. Chem. A 102, 5551–5561.

Ilan, Y., Rabani, J., 1976. On some fundamental reactions in radiation chemistry: Nanosecond pulse radiolysis. Radiat. Phys. Chem. 8, 609–611.

Ishibashi, K., Fujishima, A., Watanabe, T., Hashimotoa, K. (2000) Quantum yields of active oxidative species formed on TiO2 photocatalyst. J. Photochem. Photobiol. A 134, 139–142

25

Kakuma, Y., Nosaka, A.Y., Nosaka, Y. 2015. Difference in TiO$_2$ photocatalytic mechanism between rutile and anatase studied by the detection of active oxygen and surface species in water. Phys. Chem. Chem. Phys. 17, 18691–18698.

Kozmér, Z., Arany, E., Alapi, T., Takács, E., Wojnárovits, L., Dombi, A., 2014. Determination of the rate constant of hydroperoxyl radical reaction with phenol. Radiat. Phys. Chem. 102, 135–138.

Land, E.J., Truscott, T.G., 1979. Triplet excited state of coumarin and 4'5'-dihydropsoralen: Reaction with nucleic acid bases and amino acids. Photochem. Photobiol. 29, 861–866.

Louit, G., Foley, S., Cabillic, J., Coffigny, H., Taran, F., Valleix, A., Renault, J.P., Pina, S., (2005). The reaction of coumarin with the OH radical revisited: hydroxylation product analysis determined by fluorescence and chromatography. Radiat. Phys. Chem. 72, 119–124.

Maeyama, T., Yamashita, S., Baldacchino, G., Taguchi, M., Kimura, A., Murakami, T., Katsumura, Y., 2011a. Production of a fluorescence probe in ion-beam radiolysis of aqueous coumarin-3-carboxylic acid solution–1: beam quality and concentration dependences. Radiat. Phys. Chem. 80, 535–539.

Maeyama, T., Yamashita, S., Taguchi, M., Baldacchino, G., Sihver, L., Murakami, T., Katsumura, Y., 2011b. Production of a fluorescence probe in ion-beam radiolysis of aqueous coumarin-3-carboxylic acid solution—2: Effects of nuclear fragmentation and its simulation with PHITS. Radiat. Phys. Chem. 80, 1352–1357.

Manevich, Y., Held, K., Biaglow, J.E., 1997. Coumarin-3-carboxylic acid as a detector for hydroxyl radicals generated chemically and by gamma radiation. Radiat. Res. 148, 580–591.

Nagarajan, S., Skillen, N.C., Fina, F., Zhang, G., Randorn, C., Lawton, L.A., Irvine, J.T.S., Robertson, P.K.J., 2017. Comparative assessment of visible light and UV active photocatalysts by hydroxyl radical quantification. J. Photochem. Photobiol. A 334, 13–19.

NDRL/NIST solution kinetics database on the web, https://kinetics.nist.gov/solution/ last accessed: 31 July 2019.

Newton, G.L., Milligan, J.R., 2006. Fluorescence detection of hydroxyl radicals. Radiat. Phys. Chem. 75, 473–478.

Nosaka Y., Nishikawa, M., Nosaka, A.Y., 2014. Spectroscopic investigation of the mechanism of photocatalysis. Molecules 19, 18248–18267.

Pimblott, S. M., Schuler, R. H., LaVerne, J. A. 1992. Diffusion-kinetic calculations of the effect of nitrous oxide on the yields of ionic species in the radiation chemistry of water. J. Phys. Chem. 96(20), 7839–7841.

Shen, M., Shi, Y., Tao, Q., 1995. Synthesis of fluoran dyes with improved properties. Dyes Pigments 29, 45–55.

Singh, T.S., Rao, B.S.M., Mohan, H., Mittal, J.P., 2002. A pulse radiolysis study of coumarin and its derivatives. J. Photochem. Photobiol. A 153, 163–171.

Spinks, J.W.T., Woods, R.J., 1990. An introduction to radiation chemistry, 3rd edn. Wiley-Interscience, New-York.

Villegas, M.L., Bertolotti, S.G., Previtali, C.M., Encinas, M.V., 2005. Reactions of excited states of phenoxazin-3-one dyes with amino acids. Photochem. Photobiol. 81, 884–890.

Wang, C., Bahnemann, D.W., Dohrmann, J.K., 2001. Determination of photonic efficiency and quantum yield of formaldehyde formation in the presence of various TiO2 photocatalysts. Water Sci. Technol. 44, 279–286.

Weeks, J.L., Meaburn, G.M.A.C., Gordon, S., 1963. Absorption coefficients of liquid water and aqueous solutions in the far ultraviolet. Radiat. Res. 19, 559–567.

Yamashita, S., Baldacchino, G., Maeyama, T., Taguchi, M., Muroya, Y., Lin, M., Kimura, A., Murakami, T., Katsumura, Y., 2012. Mechanism of radiation-induced reactions in aqueous solution of coumarin-3-carboxylic acid: effects of concentration, gas and additive on fluorescent product yield. Free Radic. Res. 46, 861–871.

Zhang, J., Nosaka, J., 2015. Photocatalytic oxidation mechanism of methanol and the other reactants in irradiated TiO_2 aqueous suspension investigated by OH radical detection. Appl. Catal. B 166–167, 32–36.

Declaration of interests

☒ The authors declare that they have no known competing financial interests or personal relationships that could have appeared to influence the work reported in this paper.

☐The authors declare the following financial interests/personal relationships which may be considered as potential competing interests:

Declarations of interest: none

Author statement

Tünde Alapi: Conceptualization, data evaluation, organization of research work, writing-original draft preparation, reviewing and editing

Erzsébet Takács: Conceptualization, writing- original draft preparation, data evaluation, reviewing and editing

László Wojnárovits: Conceptualization, writing- Original draft preparation, data evaluation, reviewing and editing

Klára Hernádi:, Acquisition of the financial support for the project leading to this publication reviewing and editing

Máté Náfrádi: experimental work, data evaluation, writing- original draft preparation

Luca Farkas: experimental work, data evaluation

Krisztina Kovács: experimental work, data evaluation